Methodology for Flow and Salinity Estimates in the Sacramento-San Joaquin Delta and Suisun Marsh

22nd Annual Progress Report
August 2001

Chapter 5:
DSM2 San Joaquin Boundary Extension

Author: Thomas Pate

5 DSM2 San Joaquin Boundary Extension

5.1 Introduction

The purpose of the DWR DSM2 boundary extension is to create a direct dynamic link between the Delta and the state's second longest river, the San Joaquin. Many Delta water supply, water quality, and fishery issues are closely linked to conditions in the San Joaquin River (SJR). Extension of the SJR boundary will provide a tool to investigate how the Delta may respond to different SJR management strategies.

The system domain for this project is the portion of the SJR from near Vernalis to the Mendota Pool (see Figure 5-1). The project was divided into two phases because of substantial gaps in bathymetry data. Phase I is that portion of the domain from the Bear Creek confluence near Stevinson to the current boundary near Vernalis. Phase II is that portion of the domain from Stevinson to Mendota Pool. In general, the SJR boundary extension work reported herein is limited to Phase I.

5.2 Description

The SJR Basin is 290 miles long and averages about 130 miles wide, encompassing approximately 32,000 square miles, or one-fifth of California. The SJR flows west from its headwaters in the Sierra National Forest, then north along the southern Central Valley floor to the Sacramento-San Joaquin Delta.

Within the Phase I boundaries, there are three major eastside tributaries draining portions of the Sierra-Nevada western slope:

- Stanislaus River
- Tuolumne River
- Merced River

These tributaries primarily convey spring snowmelt with some rainfall runoff and agricultural drainage from the lower reaches. The water quality of these sources is generally good.

There are five tributary streams on the westside draining portions of the Diablo Coastal Range eastern slope:

- Hospital/Ingram Creek
- Del Puerto Creek
- Orestimba Creek
- Mud Slough
- Salt Slough

Rainfall runoff is relatively sparse along the eastern slope of the coastal range due to a rain shadow effect. These tributaries primarily convey agricultural drainage most of the year with some rainfall runoff during storm events. The water quality of these sources is relatively poor.

The agricultural activities influencing the SJR within the Phase I boundaries can be compartmentalized into two components:

- Eastside Agriculture
- Westside Agriculture

The eastside is fairly well organized and accountable with a small number of irrigation districts and a clearly defined plumbing system. The westside can be characterized as just the opposite.

There are only three identified municipal discharges to the SJR within the Phase I boundaries:

1. Newman Wastewater Treatment Plant
2. Turlock Wastewater Treatment Plant
3. Modesto Wastewater Treatment Plant

There are no significant industrial discharges identified within the Phase I boundaries (Kratzer et al. 1987).

5.3 Model Geometry Development

A set of USGS 7.5-minute topographic maps encompassing the project area was used to discretize the domain into 92 reaches with 93 nodes (Phase I & II). The locations of the nodes generally correspond to a hierarchy of major tributaries, possible point sources of inflow and outflow, or convenient landmarks. The geographic coordinate of each node was manually measured from the maps using the Universal Transverse Mercator, Zone 10 (UTM) reference system. The length of each reach was manually measured from the maps using a digital planimeter. Three values per reach were measured then averaged. The reaches are approximately 1 to 2 miles long.

Bathymetry data for the system domain were obtained from the U.S. Army Corps of Engineers (USACE). The data were transformed from the latitude/longitude coordinate system to the UTM coordinate system using "Corpscon," public domain software developed by USACE. The transformed bathymetry data and nodal coordinates were then input into DWR's Cross Section Development Program (CSDP).

CSDP was used to define the system geometry, such as channel alignment and cross sections, for input to DSM2. The model's river reaches were defined by aligning centerlines to follow the thalweg (low flow channel) that was visually located from the bathymetry data graphically displayed in CSDP. A new function was added to CSDP that calculates the reach length from the aligned centerlines. However, special care is necessary for this function to give sufficient results. The thalweg can be difficult to visually extract from the data and is highly sinuous. The placement of many short centerline segments may be necessary to accurately define a meandering channel alignment. Many short segments were used to describe the channels in

CSDP. As a benchmark, the reach lengths computed by CSDP were compared to the manual planimeter measurements. The total net difference overall between the two methods was approximately 2 feet, with CSDP yielding the greater length.

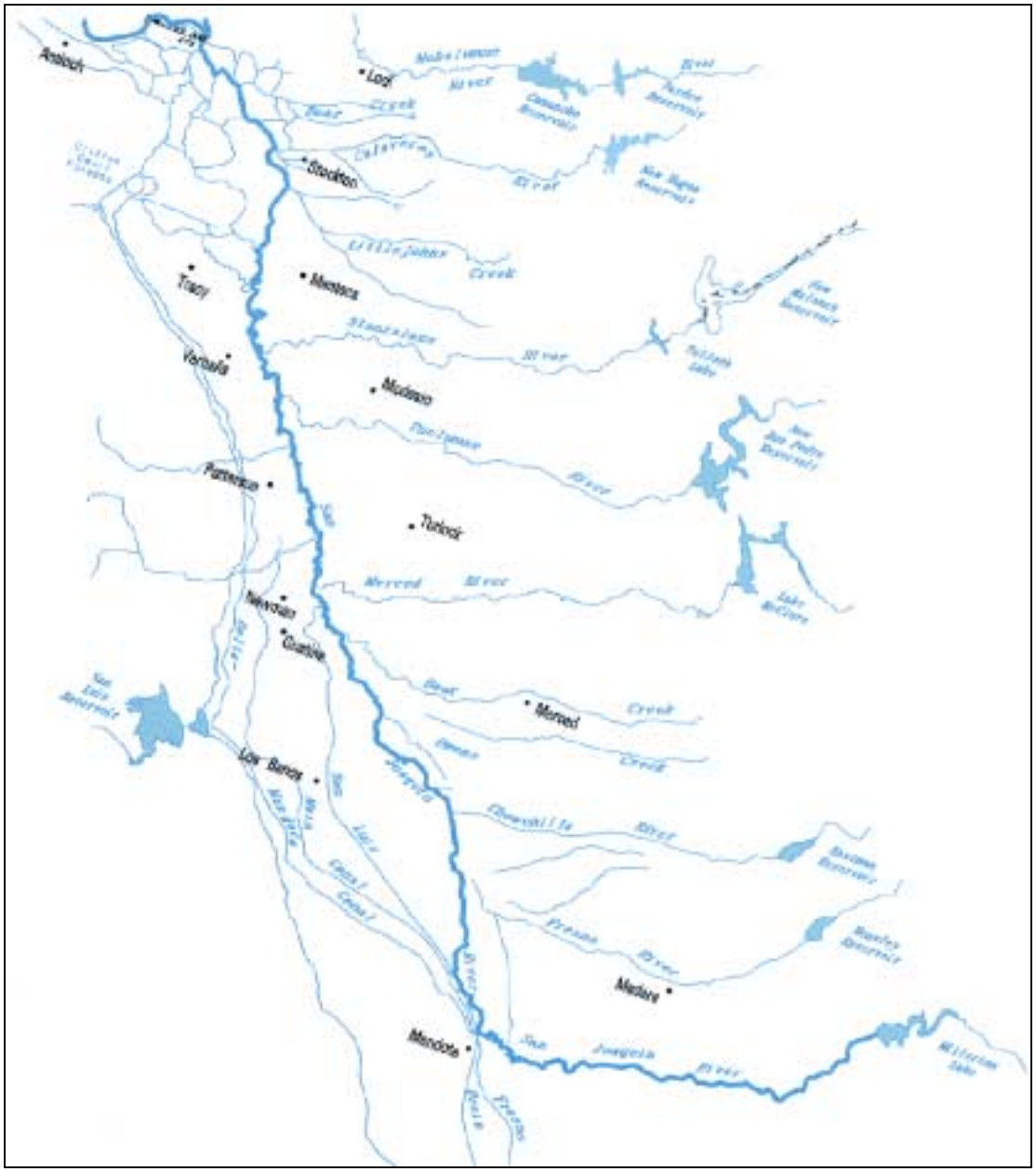

Figure 5-1: San Joaquin River.

Irregular cross sections were developed using CSDP to approximate the river's existing natural shape. Every channel has at least one representative irregular cross section and some have as many as three. Engineering judgement was used to distinguish a realistic cross section from the bathymetry data displayed near chosen locations. In most cases, the thalweg of the cross section was well defined but the floodplain was not. Digital aerial photos were used to reasonably approximate the shape and extent of the flood plains.

Even with the use of irregular cross sections, DSM2 still requires the definition of two rectangular cross sections per channel segment. These rectangular cross sections are only used if there is not at least one irregular cross section in a given channel segment. Therefore, a homogeneous rectangular cross section width of 500 feet was specified at the upstream and downstream sides of each node with a linear bottom slope between nodes. The slope was calculated using the change in channel elevation from the upstream boundary near Stevinson to Vernalis, approximately 60 feet (msl) to 0 feet (msl), respectively, divided by the number of reaches between those locations. A stage of 12 feet above the bottom elevation was specified for the initial condition.

5.4 Geometry Refinement

A mock planning study was developed for the model's first trial run.. The purpose of this exercise was to test the planning mode input files and new geometry for design flaws. A few select periods with hydrologic conditions representative of dry, normal, and wet scenarios were chosen. The hydrology for the Delta and major SJR tributaries was obtained from the DWR Planning Simulation Model (DWRSIM). Agricultural consumptive use was not readily available for the SJR and was neglected for these preliminary simulations.

The major problem encountered in the first trial run was posed by channels drying up for the dry hydrologic scenario. DSM2 will not allow a discontinuity in the flow regime and model calculations will not proceed if a channel dries up. This error can typically be attributed to large changes in cross sectional area or dramatic changes in bottom elevation between irregular cross sections.

A systematic approach was developed to debug the geometry design. The model was run until a channel segment dried up, then the irregular cross section(s) associated with that channel segment was (were) removed and the model run again. If no irregular cross sections are defined for a given channel segment, then the model will default to the rectangular cross section defined for that channel segment. This process was repeated until the model ran to a successful completion. Approximately 40 percent of the irregular cross sections was removed, most of them consecutive and localized to four general areas. This consecutive and highly localized trend suggested that not all of the cross sections removed were problematic.

The bottom elevation of a default rectangular cross section in one channel segment may not closely match the bottom elevation of an irregular cross section in a neighboring channel. This requires the introduction of a continuous block of rectangular cross sections where the elevations of the upstream and downstream ends of this section approximate the elevations of the neighboring irregular cross sections. Also, a problematic cross section may not cause an error in its own channel segment, but may cause an error in other channel segments in close proximity. In some cases where a channel segment had multiple cross sections, only one cross section was the source of error.

Based on these conclusions, a refinement process was conducted to differentiate potentially good cross sections from the problematic ones. Each problem area was investigated independently of the others. Irregular cross sections were reintroduced and removed in systematic combinations

until only a minimal number of irregulars were necessary to be removed to achieve a completed run. This process reduced the number of likely problematic cross sections to approximately 35 percent.

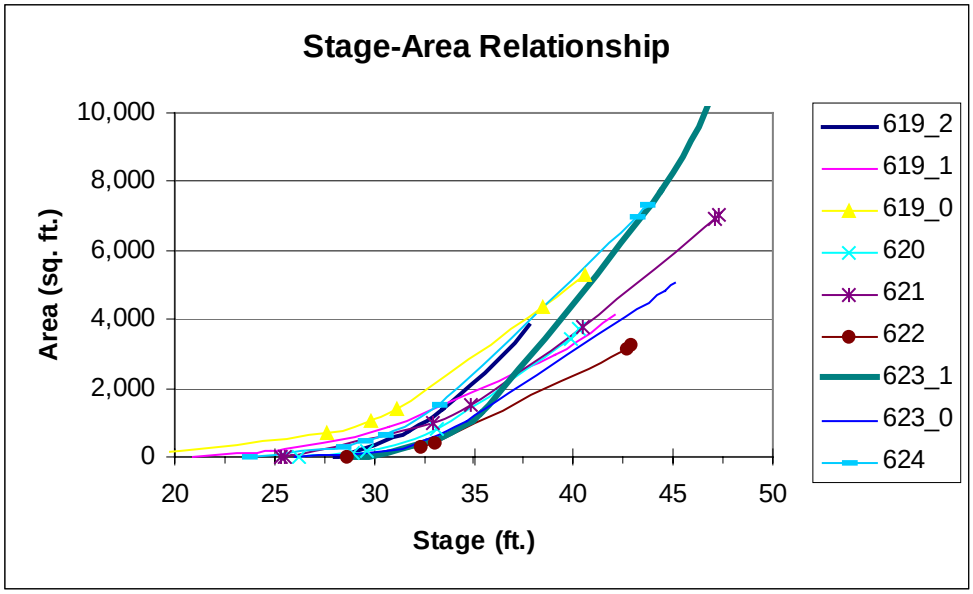

Figure 5-2: Stage-Area Relationship for Channels 619 to 624.

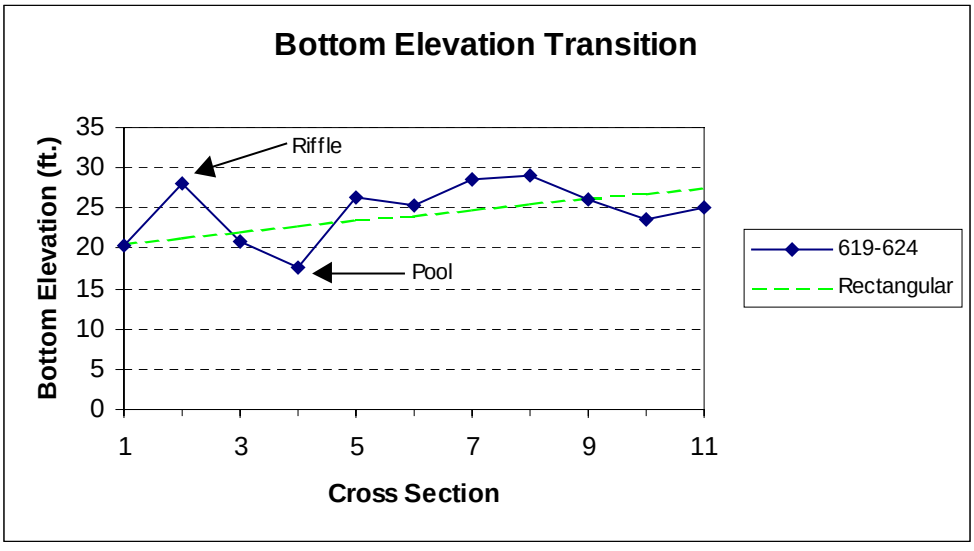

Figure 5-3: Bottom Elevation Transition for the Irregular Cross Sections from Channels 619 to 624.

The next step was to determine which cross section was the likely source of the problem. Two visualization methods were applied. The first method was to plot a family of stage to cross sectional area relationship curves for both the problematic cross section and a few cross sections upstream and downstream of that location (see Figure 5-2). The other method was to sequentially plot the bottom elevations of a problematic cross section and a few neighboring

cross sections (see Figure 5-3). These tools were valuable assets in determining which geometric attribute was most likely causing the problem. In all cases, the bottom elevation transition was found to be the problem. The model generally experienced channel drying with changes in elevation greater than 5 feet between cross sections.

Some of the deep pools and shallow riffles needed to be averaged. The bottom elevations of the corresponding rectangular cross sections were superimposed on a "bottom elevation transition" plot such as shown in Figure 5-3. This provided a reference baseline to a working slope since the model ran successfully when those cross sections were used as substitutes. The bathymetry data were revisited to determine a better location in the channel to draw a representative cross section with a bottom elevation closer to this baseline. In a few cases where a channel had more than one irregular cross section, a surplus section was deleted when relocation failed. After some iteration, the model ran to a successful completion without substitution of rectangular cross sections.

5.5 Historical Study Development

A historical study was developed to calibrate the DSM2 model extension for the HYDRO and QUAL modules. Flow (cfs) and stage (Feet, MSL) were simulated for HYDRO and salinity (EC) for QUAL. The concept of the historical study is to run the model using historical data as the boundary conditions and compare simulated model results to known historical observations.

5.5.1 Development of Boundary Conditions

A mass balance water quality model known as the San Joaquin River Input-Output (SJRIO) model was originally developed by the California State Water Resources Control Board (SWRCB) and University of California, Davis (UCD) staff. SJRIO has been extensively tested and calibrated (Kratzer et al., 1987) and is currently used by Central Valley Regional Water Quality Control Board (CVRWQCB) and the San Joaquin River Management Program Water Quality Subcommittee (SJRMP-WQS) for water quality predictions. The SJRIO model code, documentation, its developers, and current users were consulted in developing the first-cut boundary conditions for DSM2. The intention was to mimic the source and sink locations and types as closely as possible, and use the assumptions utilized by SJRIO where other data sources could not be located. The following SJRIO model components were considered in the development of DSM2 boundary conditions:

- SJR at Lander Avenue, the upstream boundary
- Three eastside tributaries: Stanislaus R., Tuolumne R., Merced R.
- Five westside tributaries: Hospital/Ingram Cr., Del Puerto Cr., Orestimba Cr., Mud and Salt Sloughs
- Appropriative and riparian diversions from the SJR and eastside tributaries
- Surface agricultural discharges, including tail water and operational spills
- Subsurface agricultural discharges
- Municipal discharges
- Natural groundwater accretions or depletions

The evaporation, precipitation, and riparian vegetation water-use components were neglected. SJRIO development, boundary conditions, and assumptions are described in detail by Kratzer et al., 1987.

Research for the best available sources of data was conducted in conjunction with the SJRMP-WQS. In general, there are two types of data: observed or empirical. Six data sources were identified to fulfill the DSM2 boundary data needs and are summarized in Table 5-1.

Table 5-1: Summary of Data Sources for DSM2 Boundary Conditions.

Source	Type	Interval
California Data Exchange Center (CDEC)	Real-Time Monitoring	Hourly
United States Geological Survey (USGS)	Real-Time Monitoring	15 Minute
United States Bureau of Reclamation (USBR)	Historical CVP Operation	Monthly
Local Agencies	Historical Operation	Monthly
CVRWQCB	Historical Grab Sample	Weekly
SJRIO	Empirical Relationship	Variable

These sources are listed in order of desirability due to reliability, time scale interval, and availability. CDEC and USGS are best due to availability at fine time scales.

5.5.1.1 Tributaries

The observed data used to describe the DSM2 tributary boundaries for the calibration period are summarized in Table 5-2. A location map for the USGS and CDEC gauging stations is provided as Figure 5-4.

Table 5-2: Description of Current DSM2 Tributary Boundary Conditions.

Location	Description
Upper SJR	Hourly flow from the DWR SJS gauging station near Stevinson from CDEC and weekly salinity from CVRWQCB grab samples near Stevinson (Lander Avenue).
Merced River (MER)	Hourly flow from the DWR MST gauging station near Stevinson from CDEC and daily salinity from SJRIO.
Tuolumne River (TUO)	Hourly flow from the DWR MOD gauging station at Modesto from CDEC and daily salinity from SJRIO. Flow data has been shifted forward 12 hours to account for gage distance from confluence with SJR.
Stanislaus River (STA)	Hourly flow and salinity from the DWR RIP and USBR RPN gauging stations, respectively, at Ripon from CDEC. Flow data has been shifted forward 12 hours to account for gage distance from confluence with SJR.
Salt Slough (SSL)	15-min flow and hourly salinity from the USGS gauging station 11260000 at Hwy 165 near Stevinson.
Mud Slough (MSL)	Hourly flow and salinity from the USGS gauging station 11262900 near Gustine.
Orestimba Creek (ORE)	15-min flow and salinity from the USGS gauging station 11274538 at River Road near Crows Landing.
Del Puerto Creek (DPC)	15-min flow from the USGS gauging station 11274630 near Patterson. The flow station is located a considerable distance away from SJR confluence allowing drainage to enter ungaged below the station. Some of this ungaged drainage is estimated by SJRIO. Salinity is assumed to be the same as ORE.

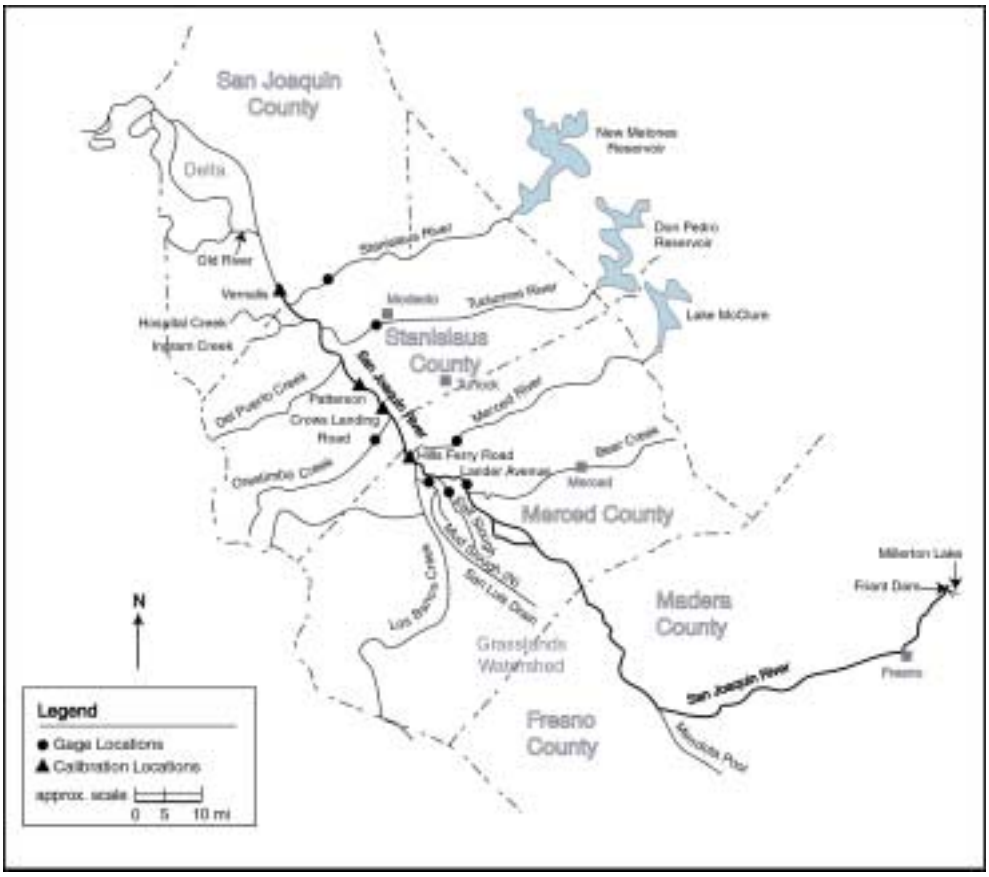

Figure 5-4: Map of Gauging Stations.

Hospital/Ingram Creek (H/I) is an ungaged watershed. Per SJRIO, flow hydrology is calculated as a percentage of ORE based on watershed size, which is approximately 64 percent. H/I salinity is also assumed to be the same as ORE due to geographic similarities.

5.5.1.2 Municipal

The City of Modesto is the only municipality that discharges directly to the SJR. The Modesto Wastewater Treatment Plant (MWWTP) maintains total monthly discharge records. The City of Turlock Wastewater Treatment Plant (TWWTP) discharges indirectly to the SJR and is accounted for later. The City of Newman Wastewater Treatment Plant (NWWTP) uses a system of retention, evaporation, and land disposal. The NWWTP only discharges to the SJR during the rainy season when the disposal site is saturated and unable to assimilate the effluent. NWWTP flow and salinity contributions to the SJR are assumed negligible (Kratzer et al. 1987).

5.5.1.3 Eastside Agriculture

Two large irrigation districts supply water for eastside agricultural (EAG) activities (see Figure 5-5). Modesto Irrigation District (MID) services the area bounded by the STA, SJR, and TUO. The area between the TUO, SJR, and MER is serviced by Turlock Irrigation District (TID). Both of these districts receive irrigation water from offstream storage sources upstream of the gages on the STA and TUO, respectively. Operational spills and agricultural tail-waters from each district are collected and conveyed by canals to point sources on the SJR, TUO, and STA.

MID has approximately 10 canals that combine and discharge to three discrete points and one spreading basin within the study boundaries:

- Lateral No. 4 (MID#4) spills to the SJR.
- Lateral No. 5 (MID#5) spills to a slough adjacent to the TUO near the SJR confluence and downstream of the MOD gauging station. This flow was assumed to reach the TUO.
- Lateral No. 6 (MID#6) spills to the STA above Koetitz Ranch and downstream of the RIP gauging station.
- Modesto Main Drain (MMAIN) conveys spills from Lateral No. 3 and 7 to Miller Lake.

Miller Lake has the ability to spill into the STA. However, no records of Miller Lake flows into the STA have been found. MMAIN spills are assumed to reach the STA by seepage, thus no time adjustments were made to the data set.

TID has approximately six canals that discharge to six discrete points within the study boundaries:

- Lateral No. 1 Spill (TID#1) spills to the TUO downstream of the MOD gauging station
- Lower Lateral No. 2 Spill (TID#2) spills to the SJR
- Lateral No. 3 Drain (TID#3), a.k.a. Westport Drain, discharges to the SJR
- Lateral No.5 Drain (TID#5), a.k.a. Carpenter Drain, discharges to the SJR
- Lateral No. 6 and 7 Spills (TID6&7) combine and spill to the SJR
- Lower Stevinson Spill (TID_LSTV) spills to the MER downstream of the MST gauging station

These six canals compound drainage from seven other canals in the TID network:

- TID#3 combines drainage from Lower Laterals (LL) #2.5 and #3
- TID#5 combines drainage from Lower Lateral Spills (LL) #4, #4.5 and #5.5
- Lateral Spills (L) #5 and #5.5. The TWWTP also discharges treated wastewater into L#5

This information was used to reconstruct portions of incomplete data sets at some discharge points when possible.

The eastside districts maintain monthly total flow records relatively close to the release points. Flow data were not available for TID#1. Some sparse salinity data were also maintained and used to determine some average "static" salinity values for quality of these sources.

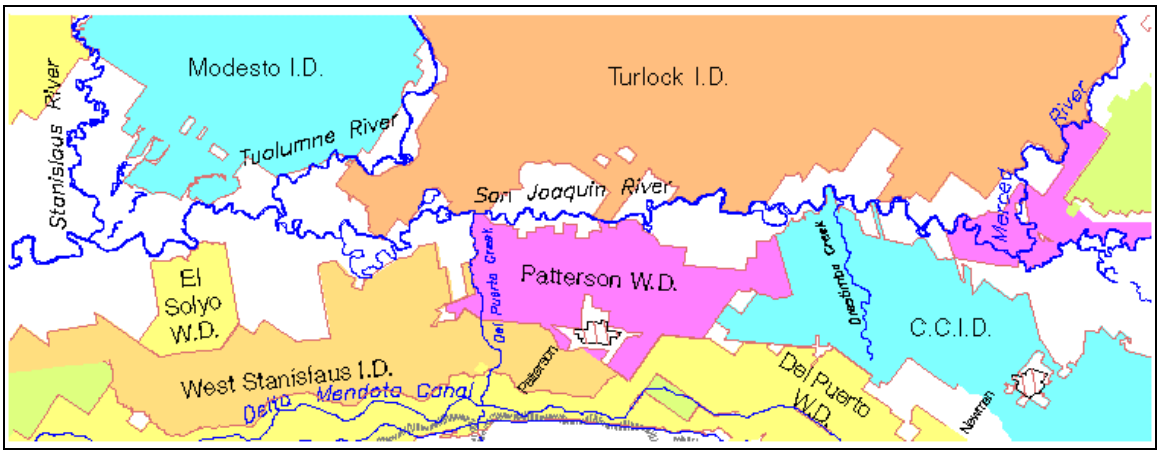

Figure 5-5: Boundaries of Relevant Public Agencies.

5.5.1.4 Westside Agriculture

Currently, five entities supply irrigation water for westside agricultural (WAG) activities (see Figure 5-5):

- El Soyo Water District (ESWD)
- West Stanislaus Irrigation District (WSID)
- Patterson Water District (PWD)
- Del Puerto Water District (DPWD)
- Central California Irrigation District (CCID)

There are three sources of water used for irrigation on the westside: SJR diversion, Central Valley Project (CVP) deliveries, and pumped groundwater. The only observed data currently available are CVP deliveries by the USBR and total monthly diversions from the SJR maintained by ESWD, WSID, and PWD. These three districts are referred to as the "BIG3" per SJRIO.

Diversion data were obtained from the BIG3 for the historical simulation period. Other districts' diversions are estimated by river mile using a relationship developed for SJRIO (Kratzer et al. 1987). This formulation is based on applying monthly average usage to maximum allowable diversion ratios of the BIG3 from

$$x_i^{t_a} = \frac{\sum_{t=1}^{12} Q_i^t}{Q_{\max_i}} \Rightarrow \bar{x}^{t_a} = \frac{\sum_{i=1}^{3} x_i^{t_a}}{3}, \forall\, i,t,t_a \in \Omega \qquad \text{[Eqn. 5-1]}$$

where:

Q = flow in (AF),
$Q_{\max}$ = maximum allowable diversion,
x = annual diversion ratio,
$\bar{x}$ = average annual 'Big3' diversion ratio,
t = month,
t_a = year,
i = 'Big3' diverters, and
Ω = time/space domain.

The maximum allocations of the other districts are distributed to assigned river miles by

$$Q_j^{t_a} = \left[\frac{Q_{\max_j}}{12}\right] \bar{x}^{t_a}, \forall\, j,t_a \in \Omega \qquad \text{[Eqn. 5-2]}$$

$$Q_j^t = \left[\sum_{i=1}^{3} \frac{Q_i^t}{Q_i^{t_a}}\right] Q_j^{t_a} \lambda_j^t, \forall\, j,t \in \Omega \qquad \text{[Eqn. 5-3]}$$

where:

j = SJRIO river mile, and
λ = month of use.

The SJRIO river mile to DSM2 node and af to cfs conversion function is

$$\hat{Q}_n^t = \xi \sum_{j}^{\forall j \in n} Q_j^t, \forall\, n,t \in \Omega \qquad \text{[Eqn. 5-4]}$$

where:

$\hat{Q}$ = flow (cfs),
n = DSM2 + SJR node, and
ξ = acre - ft $\rightarrow$ cfs conversion.

In addition to the five appropriative diverters, there are also riparian diverters whose diversion rights precede formal agreements. These diversions are ungaged and estimated by river mile from assumed acreage, crop type, and crop water demand per SJRIO (Kratzer et al. 1987) as

$$Q_i^t = \sum_{j=1}^{3} \frac{A_{ij} h_j^t}{12}, \forall\, i,t \in \Omega \qquad \text{[Eqn. 5-5]}$$

$$\hat{Q}_n^t = \xi \sum_{i}^{\forall i \in n} Q_i^t, \forall\, n,t \in \Omega \qquad \text{[Eqn. 5-6]}$$

where:

A = crop acreage,
h = water applied to crop (inches),
i = SJRIO rivermile, and
j = crop type.

The crops for the riparian users are almonds, corn, and pasture. Cropping patterns are assumed to remain the same throughout the calibration period.

Agricultural return flows are estimated by applying an efficiency factor to all of the sources of irrigation water by river mile. The tail-water typically totals 30 percent of the water supplied per source. The return calculation has four components contributing to tail-water flows per SJRIO (Kratzer et al. 1987): CVP deliveries to appropriative districts, the BIG3 SJR diversions, all other SJR diversions, and groundwater pumped from shallow aquifers. These components are combined to estimate the WAG return flows to the SJR as

$$Q_{R_i}^t = \sum_{j=1}^{10} Q_{CVP_{ij}}^t X_{CVP_{ij}} + \sum_{l=1}^{3} Q_{BIG_{il}}^t X_{BIG_{il}} + \sum_{m}^{\forall m \in i} Q_{DIV_{im}}^t X_{DIV_{im}} + \sum_{k=1}^{13} \left(Q_{GW_k}^{t_y} Y^t \right) X_{GW_{ik}}, \forall\, i,t \in \Omega \qquad \text{[Eqn. 5-7]}$$

$$\hat{Q}_{R_n}^t = \xi \sum_{i}^{\forall i \in n} Q_{R_i}^t, \forall\, n,t \in \Omega \qquad \text{[Eqn. 5-8]}$$

where:

R = drainage return,
X = return factor (%),
Y = temporal distribution (%),
CVP = Central Valley Project deliveries,
BIG = 'Big3' diversions,
DIV = other SJR diversions,
GW = groundwater pumping,
i = SJRIO river mile,
j = water/irrigation district,
k = township,
l = 'Big3' diverter,
m = SJR diverter, and
t_y = similar year type.

USBR maintains records of CVP deliveries to the districts. The CVP component was originally based on 10 appropriative districts; however, DPWD acquired six of the 10 in 1995. Since the simulation period is post-1995, the DPWD deliveries needed to be synthetically redistributed to maintain the original assumption of 10 districts. This was achieved by computing the historical average percent of the total DPWD and other six districts among each individual district from data prior to 1995. The historical average percent was then used to divide up the DPWD deliveries after 1995 into pseudo water districts to mimic the original 10. It is assumed that post-1995 geographical water use remains consistent with pre-1995 usage.

Groundwater pumping is estimated using information from USGS. Annual groundwater pumped for 13 townships along the SJR in the project area for water years 1961 to 1977 was originally based on consumptive use of water and power consumption records (Kratzer et al. 1987). The average of each of the four water year types: critically dry, dry, normal, and wet, are used based on the simulation year type in DSM2 per SJRIO.

As previously mentioned, diversions by the BIG3 are known and all other diversions are estimated. The return factors for each of the four sources per river mile was obtained from SJRIO and Kratzer et al., 1987.

The salinity of the WAG agricultural return flows is estimated using a flow-weighted mass balance for each source contribution to a node defined as

$$C_n^t = \frac{\left[\sum_{j}^{\forall j \in n} \hat{Q}^t_{R_{CVP_{jn}}}\right]\left(C^t_{CVP} + C'\right) + \left[\sum_{k}^{\forall k \in n} \hat{Q}^t_{R_{SJR_{jn}}}\right]\left(C^t_{SJR} + C'\right) + \left[\sum_{l}^{\forall l \in n} \hat{Q}^t_{R_{TRB_{nl}}}\right]\left(C^t_{TRB} + C'\right) + \hat{Q}^t_{R_{GW_n}} C_{GW}}{\left[\sum_{j}^{\forall j \in n} \hat{Q}^t_{R_{CVP_{jn}}} + \sum_{k}^{\forall k \in n} \hat{Q}^t_{R_{SJR_{jn}}} + \sum_{l}^{\forall l \in n} \hat{Q}^t_{R_{TRB_{nl}}} + \hat{Q}^t_{R_{GW_n}}\right]}, \quad \text{[Eqn. 5-9]}$$

$$\forall\, n, t \in \Omega$$

where:

C = conservative constituent concentration,
C' = degradation concentration,
CVP = Central Valley Project contribution,
SJR = SJR diversion contribution,
TRB = eastside tributary diversion contribution,
GW = groundwater pumping contribution,
j = water/irrigation district,
k = SJR diversion, and
l = eastside tributary diversion.

Each source has a different initial quality. Historical salinity data are available for the STA, SJR, and CVP. The TUO, MER, and GW are assumed to have static EC values of 150, 150, and 1000 umhos/cm, respectively. The initial concentration is increased to account for degradation from agricultural activities. A degradation concentration of 150 umhos/cm was used per SJRIO.

Some salinity data were obtained directly from SJRIO and converted from TDS to EC units using a TDS:EC ratio of 0.64 when necessary.

In addition to these returns, there are also nine tile drains on the westside that discharge directly to the SJR. These subsurface drains carry percolated irrigation water that is characterized by low flow and high salinity. Static annual flow and salinity values for each drain were obtained directly from SJRIO. The basis for these values are described by Kratzer et al., 1987.

5.5.1.5 Groundwater

In the original formulation of SJRIO, groundwater accretions and depletions were calculated using a steady-state, 1-dimensional deterministic model based on the Dupuit-Forchheimer assumptions. Groundwater flows to the SJR were calculated monthly per river mile for water years 1979, 1981, 1982, 1984, and 1985. Flows to the eastside tributaries were calculated monthly for the entire reach below the gauging stations to their confluence with the SJR. The details of the groundwater model are described in Kratzer et al., 1987. The results of the groundwater model are given as monthly and annual flow summaries.

The mean monthly groundwater flows were used to create static annual set of monthly distribution ratios by

$$\alpha^{t_m} = \frac{\overline{Q}^{t_m}}{\sum_{t_m=1}^{12} \overline{Q}^{t_m}}, \forall\, t_m \in \Omega \qquad \text{[Eqn. 5-10]}$$

where:

α = monthly mean flow distribution,
$\overline{Q}$ = average flow (AF)
t_m = month of mean year, and
i = SJRIO river mile.

The distribution ratios are then used to distribute the annual groundwater flows to the SJR per river mile by

$$\overline{Q}_i^{t_m} = \alpha^{t_m}\, \overline{Q}_i, \forall\, t_m, i \in \Omega \qquad \text{[Eqn. 5-11]}$$

$$\hat{Q}_n^{t_m} = \xi \sum_{i}^{\forall i \in n} \overline{Q}_i^{t_m}, \forall\, t_m, n \in \Omega \qquad \text{[Eqn. 5-12]}$$

The same formulation given by equations 5-10, 5-11, and 5-12 is used for the tributaries STA, TUO, and MER, except without the "i" subscript. The result yields a set of mean monthly groundwater flows that vary spatially and monthly but are constant on an annual basis. The current version of SJRIO does not use this formulation.

The salinity values associated with the groundwater were obtained from Kratzer et al., 1987. A static salinity is assigned based on river mile.

The necessary boundary conditions for the Delta portion used for the DSM2 simulations were previously developed by the Delta Modeling Section.

5.5.2 Calibration Procedure

The methodology for hydrodynamic calibration is to systematically vary the model parameters for channel roughness, Manning's 'n', throughout the model domain until the "best" convergence between the model output and the historical data is achieved. For the SJR above Vernalis, water quality calibration can only be achieved through boundary input manipulation. The dispersion coefficient has no effect due to the lack of tidal influence upstream of Vernalis. An initial value of 0.035 was chosen for channel roughness and 0.2 for the dispersion coefficient for all channels upstream of Vernalis. These parameter values for DSM2 channels below Vernalis were consistent with DSM2 Calibration Run #49 from the IEP DSM2 Project Work Team calibration effort (see Chapter 2).

Four calibration stations (see Figure 5-4) were selected within the Phase I domain for comparison benchmarks:

- SJR near Newman, Hills Ferry Road Bridge (NEW), flow only
- SJR at Crows Landing Road Bridge (CLB), flow and salinity
- SJR at Patterson Bridge (SJP), flow only
- SJR near Vernalis at Airport Road Bridge (VER), flow and salinity

These locations were chosen because reliable gauging stations that are independent of the model results are present there and are listed in succession from upstream to downstream. All four stations provide data for stage and flow, but only two have corresponding salinity data.

From a thorough review of these data sources, a calibration simulation time window was chosen. The period of May, 1997 through September, 1999 was selected due to the most comprehensive availability of data at all boundaries.

Stage, flow, and salinity at the four calibration locations were obtained from the HYDRO and QUAL runs, respectively, for the calibration period. The model output was compared to the observed data using time series and error plots for each location. The mean sum of the squared residuals (MSS) was also computed for all acceptable observed values, as

$$e = \sqrt{\frac{\sum_{i=1}^{n}\left(\hat{Y}_i - Y_i\right)^2}{n}} \qquad \text{[Eqn. 5-13]}$$

where:

$e = \text{MSS},$
$Y = \text{observed value},$
$\hat{Y} = \text{model estimated value, and}$
$n = \text{accepted values of } Y$

The MSS calculates the average deviation (error) of the model simulation from the observed data and was used as a benchmark to detect subtle differences between successive model calibration runs.

5.5.3 Pre-Calibration Results

A series of approximately 15 HYDRO preliminary calibration runs have been conducted to date. QUAL was run in conjunction with HYDRO beginning with the 10th run. Refinement of the boundary conditions and assumptions were conducted for each successive pre-calibration run until the point of diminishing return was reached. HYDRO Run14a and QUAL Run14 correspond to the best effort pre-calibration model runs given the best available historical data and derived relationships.

5.5.3.1 HYDRO

In general, the HYDRO results showed good trending with the field observations. As flood waves moved through the system, the model properly simulated the rise and fall of the observed hydrographs at the calibration stations. There are usually two annual characteristic flow regimes that occur on the SJR: a high-flow regime during the winter and spring storm season, and a low-flow regime during the summer and fall. The chosen calibration period contains an extreme flood season (1998) and a moderate (1999) one. The model performance was typically good during the low-flow regime (less than 5,000 cfs). However, the model did not perform as well for the high-flow regime from approximately February 1998 through July 1998. The magnitude and phase of the flood waves were typically missed during this period. The model's estimated flood peaks were over- and underestimated inconsistently between the calibration locations. The model's phase consistently lead the observed flood peaks. This phase shift can be distinguished as abrupt spikes on the residual plots that accompany the calibration results for each calibration station below. The MSS residual at the calibration locations increased in the downstream succession, with the greatest propagation of error occurring at VER.

Modeled stage at NEW was typically a good match to the observed data (see Figure 5-6). The model slightly overestimated for the majority of the simulated period. The difference between the modeled and observed flood peak stage was approximately 0.3 feet and averaged about 1.5 feet throughout the high-flow period. Some divergent behavior was exhibited toward the tail end of the simulation period from approximately March 1999 to the end of the simulation period.

DSM2 overestimated stage at CLB during the low-flow period and underestimated during the high-flow period (see Figure 5-7). The difference between the modeled and observed flood peak stage was approximately 1.5 feet. Divergent behavior was also exhibited at this location during the same period.

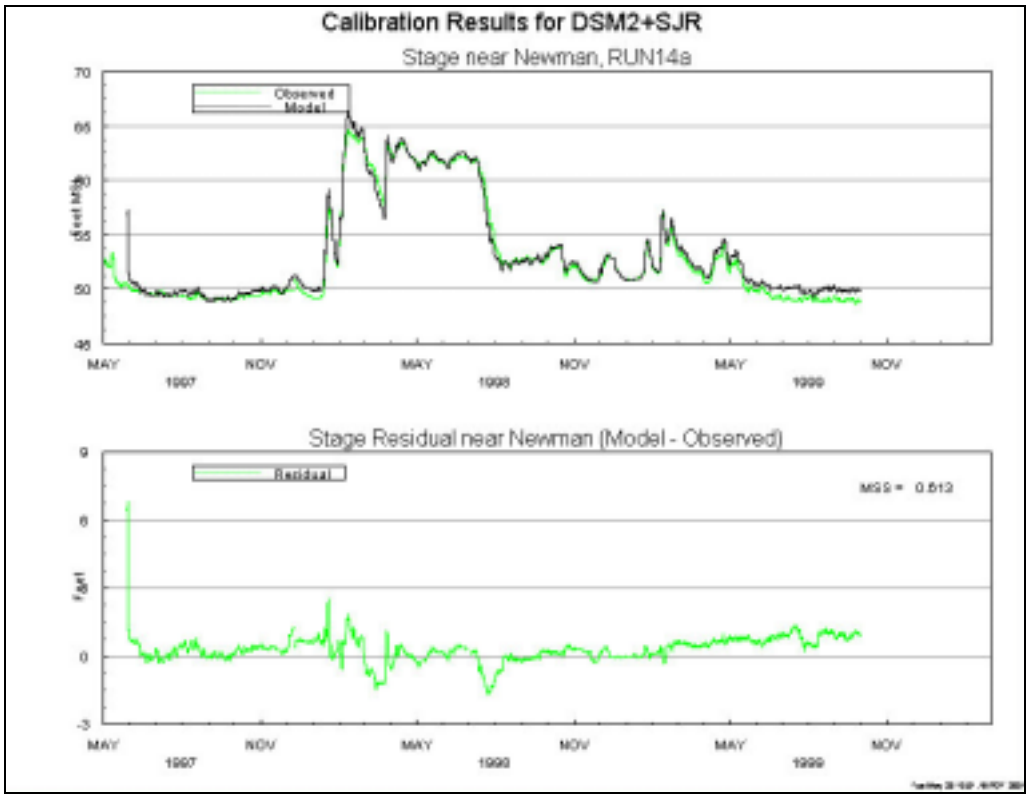

Figure 5-6: DSM2 Pre-Calibration Results for Stage at NEW.

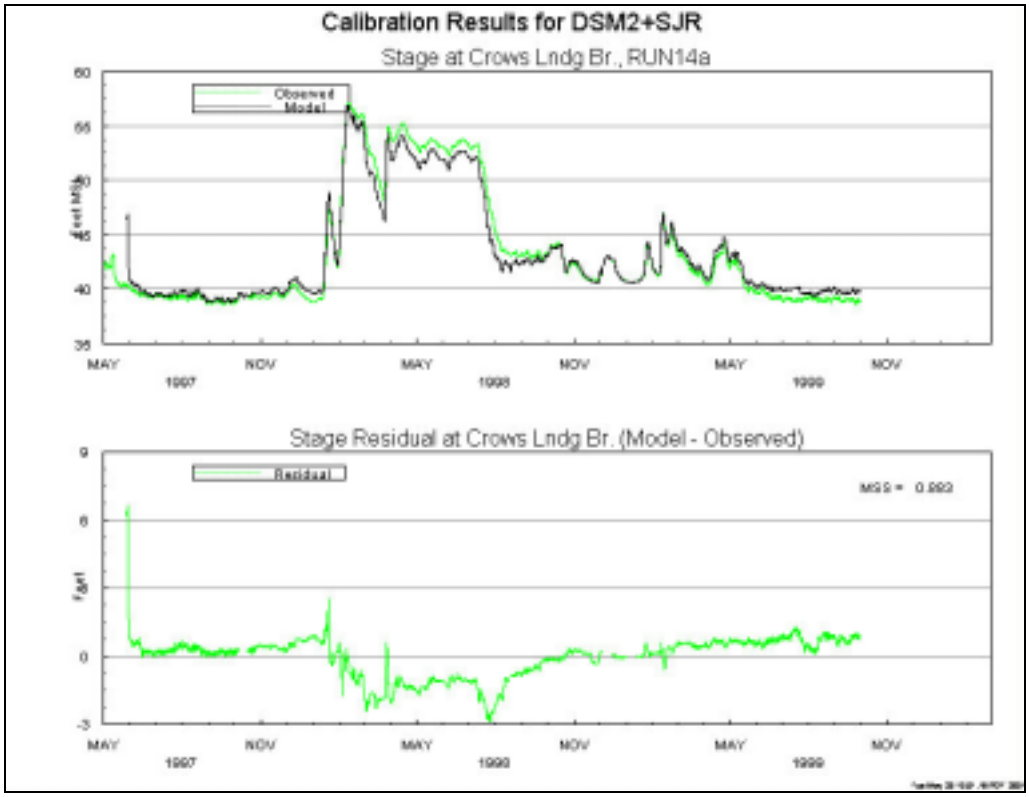

Figure 5-7: DSM2 Pre-Calibration Results for Stage at CLB.

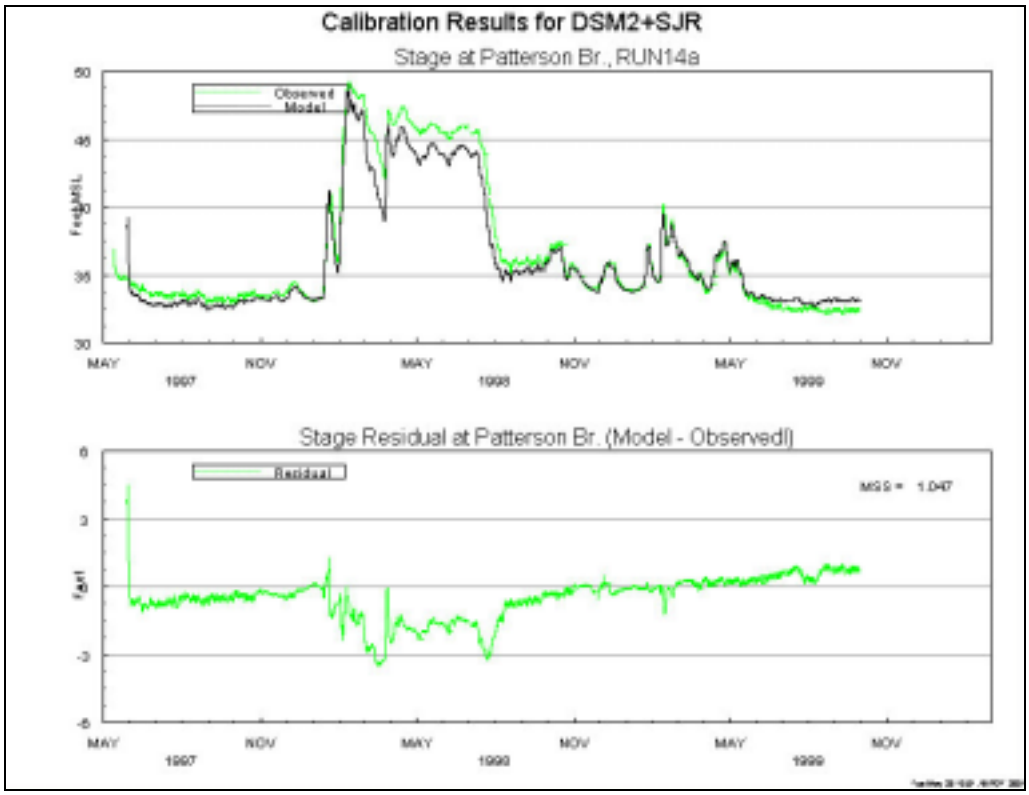

Figure 5-8: DSM2 Pre-Calibration Results for Stage at SJP.

Modeled stage at SJP was underestimated from the beginning of the simulation period through November 1998, and then was overestimated for most of the remaining period (see Figure 5-8). The difference between the modeled and observed flood peak stage was approximately 0.5 feet and averaged about 1.5 feet throughout the high-flow period. Divergent behavior was also exhibited at this location during the same period as at NEW and CLB.

Stage at VER was generally underestimated throughout the majority of the simulation period (see Figure 5-9). The difference between the modeled and observed flood peak stage was approximately 0.5 feet. An average deficiency of about 1.5 feet was exhibited from the beginning of the simulation period through the first low-flow period. As the simulation approached the high-flow period, the model simulation converged toward the observed data. The period from approximately July 1999 to the end of the simulation, the last low-flow period, exhibited an average deficiency of about 0.75 feet with divergent behavior.

In general, DSM2 stage was a good match to the observed data at NEW, CLB, and SJP during the period from November 1998 to March 1999. The front-end and tail-end divergence magnitudes increased in the downstream station progression.

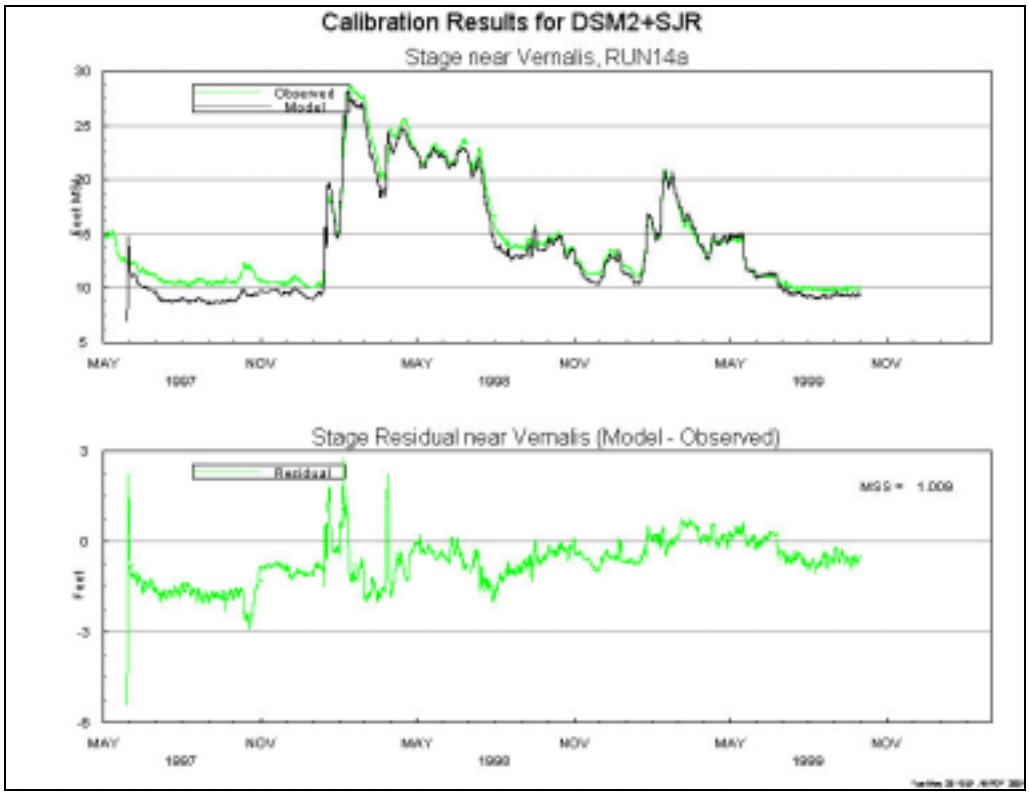

Figure 5-9: DSM2 Pre-Calibration Results for Stage at VER.

Modeled flows at NEW and CLB were an excellent match to the observed flows during the low-flow periods (see Figures 5-10 and 5-11). The model's simulation typically overestimated at NEW and consistently underestimated at CLB. The difference between DSM2 and the observed flood peaks was approximately +2,000 cfs and –3,500 cfs for NEW and CLB, respectively, with DSM2 leading the observed results. The phase shift was approximately eight hours and 15 hours, respectively.

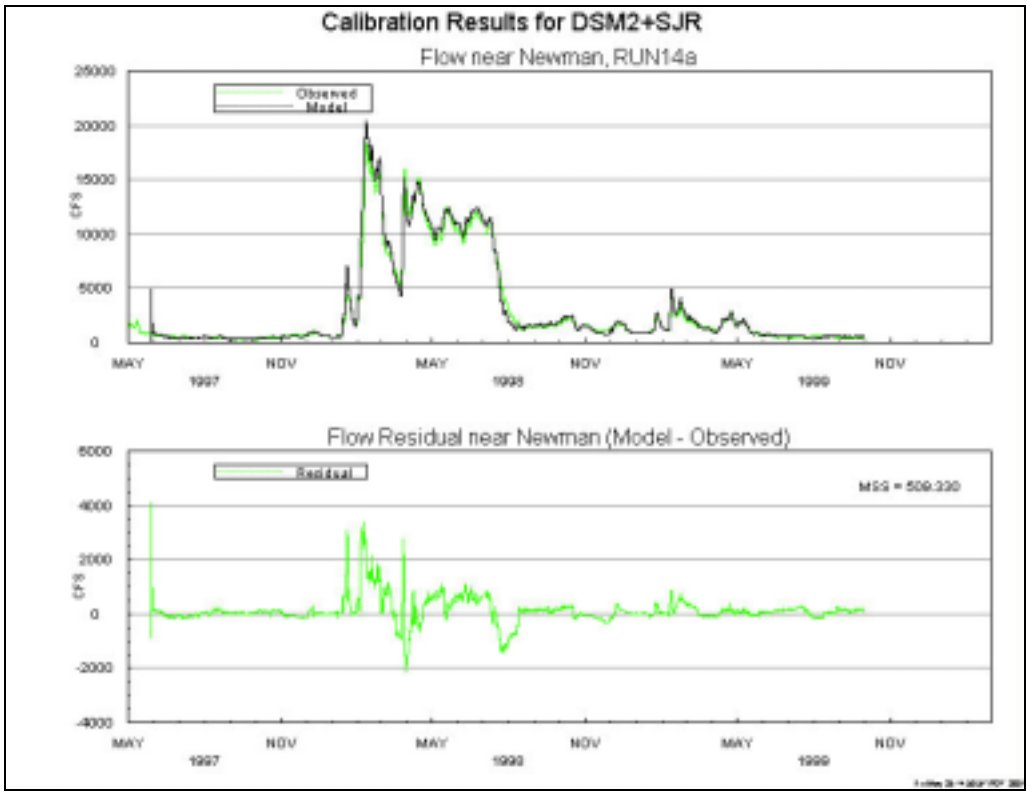

Figure 5-10: DSM2 Pre-Calibration Results for Flow at NEW.

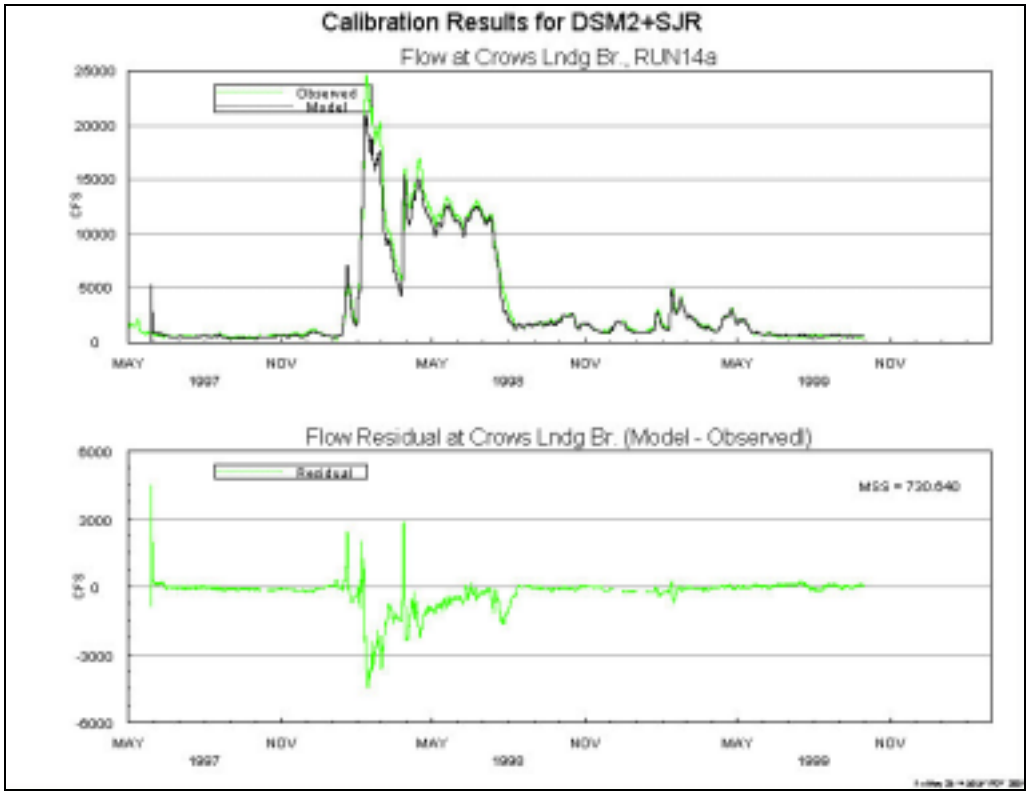

Figure 5-11: DSM2 Pre-Calibration Results for Flow at CLB.

DSM2 generally underestimated the flows during the low-flow period (see Figures 5-12 and 5-13) at SJP and VER. During the high-flow period, flows at SJP and VER were mixed. The magnitude of the flood peak at SJP was overestimated by approximately 2,500 cfs. The largest phase shift at SJP did not occur at flood peak but ranged from 16 to 24 hours at secondary peaks. The magnitude of the flood peak at VER was underestimated by approximately 700 cfs and exhibited a phase shift of approximately 70 hours (see Figure 5-14).

In general, modeled flow was very good at NEW, CLB, and SJP during the period from November 1998 to March 1999. The low-flow regime modeled flow deficit increased with the progression of stations downstream.

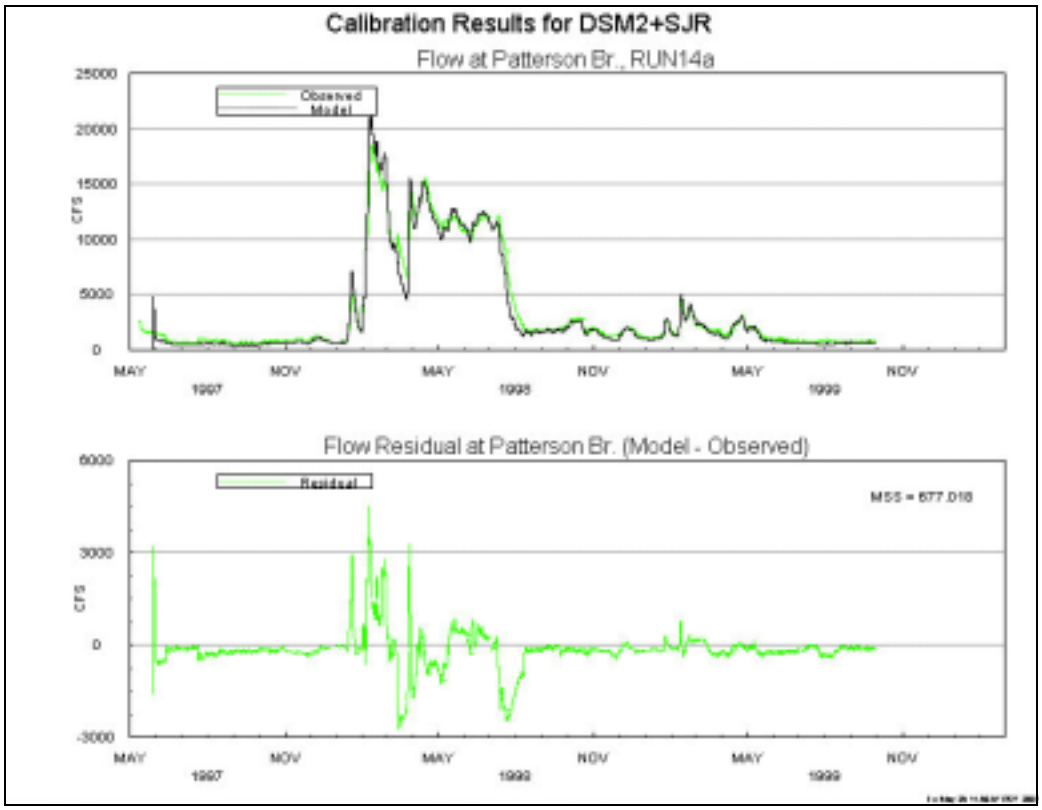

Figure 5-12: DSM2 Pre-Calibration Results for Flow at SJP.

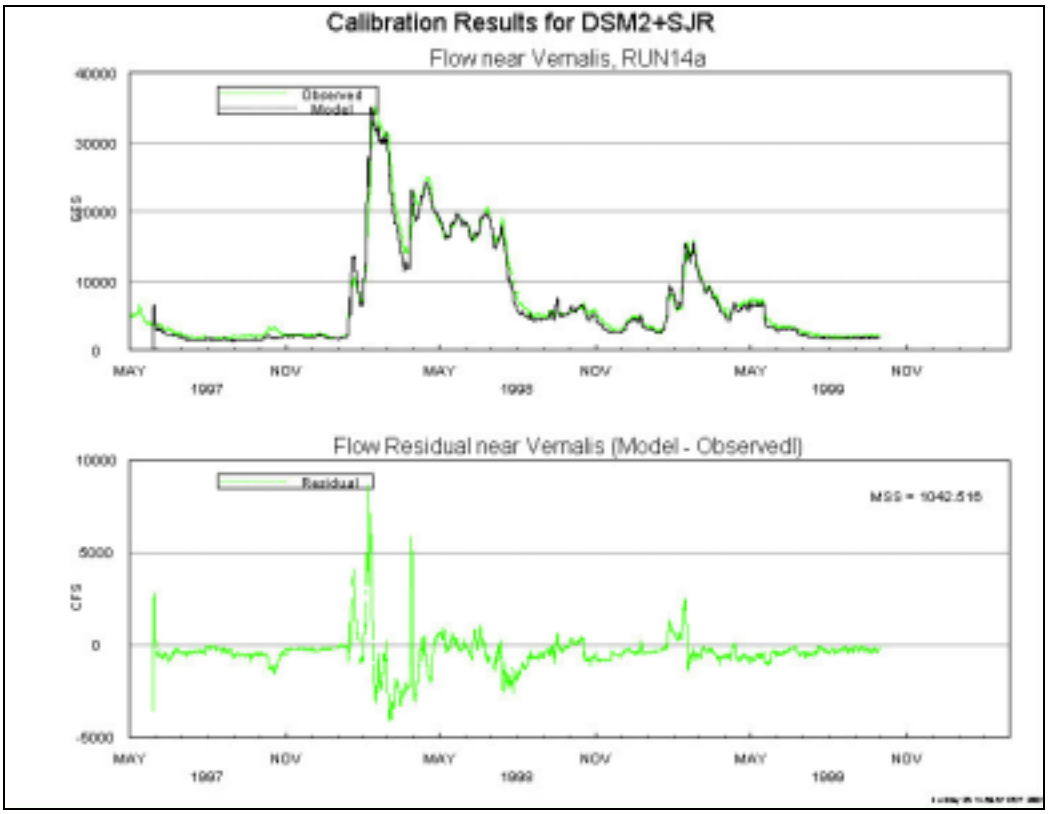

Figure 5-13: DSM2 Pre-Calibration Results for Flow at VER.

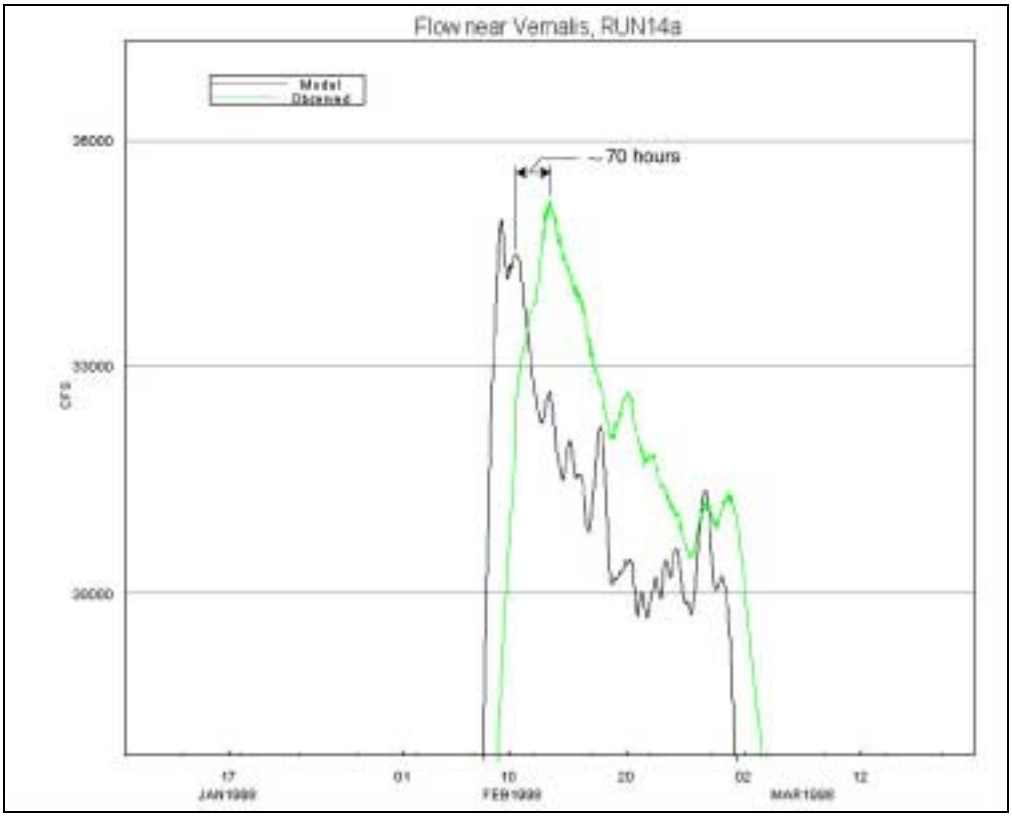

Figure 5-14: Example of Flood Peak Phase Shift at VER.

5.5.3.2 QUAL

In general, the QUAL results showed good trending with the field observations. As poor quality flows moved through the system, the model properly simulated the rise and fall of the observed salinity at the calibration stations. There are usually three annual characteristic salinity regimes that occur on the SJR: a low-salinity regime during the spring prior to the irrigation season; the irrigation season during the summer and fall, which contributes to a moderate-salinity regime due to irrigation tail-water; and a high-salinity regime during the winter storm season that flushes accumulated salts from the land to the river. The model performance was typically good during the low-salinity regime. However, the model did not perform as well for the high-salinity regime.

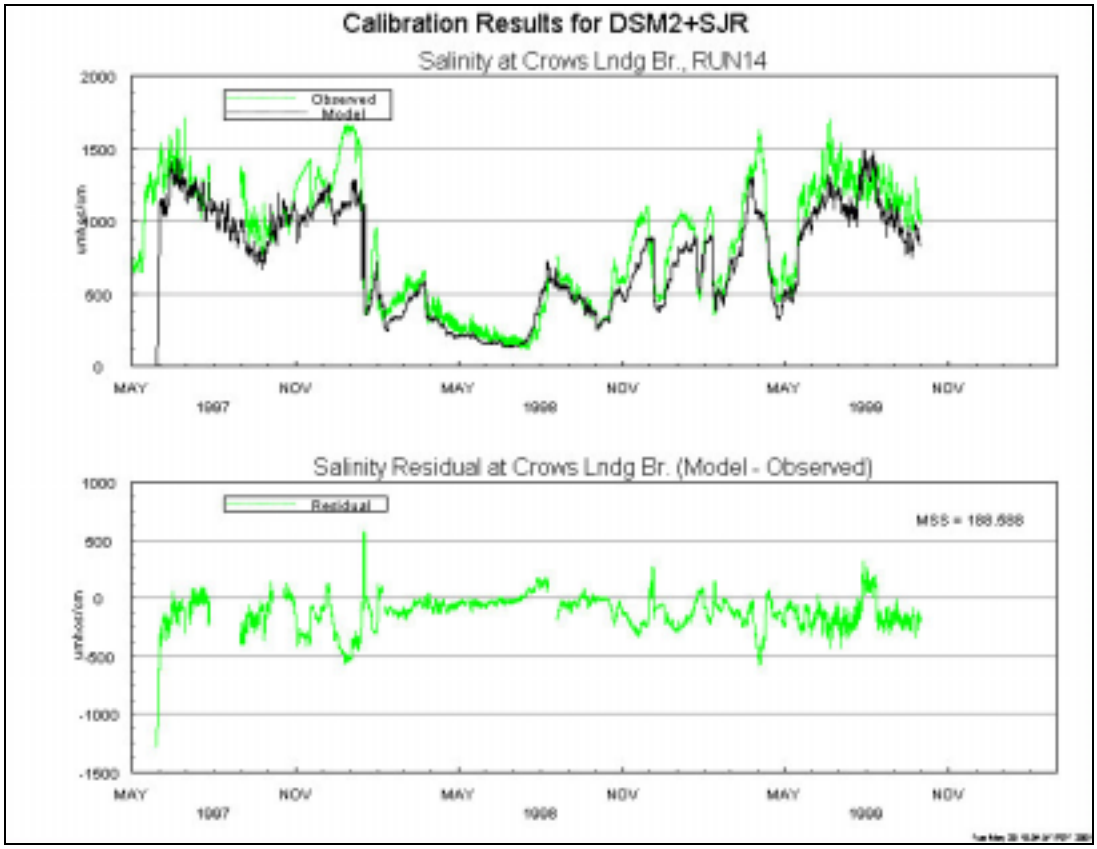

Figure 5-15: DSM2 Pre-Calibration Results for Salinity at CLB.

DSM2 generally under-predicted the salinity at CLB compared to the observed data (see Figure 5-15). The peaks during the high-salinity periods were often missed by an approximate average of 300 umhos/cm. The results were similar at VER (see Figure 5-16) except for the period from January 1998 through October 1998. During this period, the model tended to slightly over-predict the salinity.

As expected, the salinity dramatically decreased from CLB to VER. This is primarily due to contributions from the higher quality Eastside tributaries downstream of CLB, particularly the Stanislaus River.

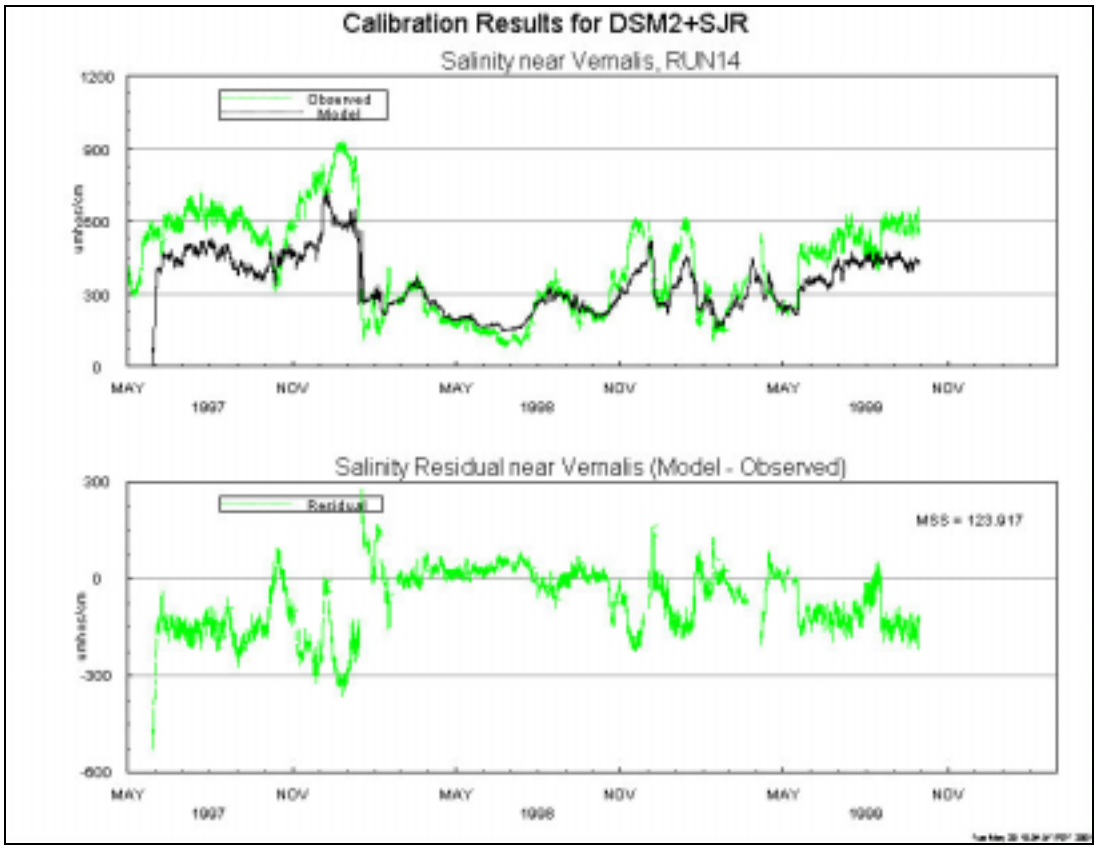

Figure 5-16: DSM2 Pre-Calibration Results for Salinity at VER.

5.5.4 Current Calibration Results

A thorough analysis of the pre-calibration model results compared to the field observations indicated that some information present in the observed data is not being reflected in the boundary conditions outlined previously.

With the exception of the high-flow regime, the simulated flow during the low-flow regime at NEW and CLB are a relatively good match. The corresponding simulated salinity at CLB could be better but the flow is already a good match. Thus, in order to improve the modeled salinity, the representation of the boundary conditions must be improved, which is difficult to do without deviating from some SJRIO assumptions.

In contrast, the low-flow regime at SJP and VER was not as good. The total average simulated flow deficit at VER is approximately 350 cfs during these periods. A closer evaluation of the pre-calibration simulation results shows that 200 of the 350 cfs occurs in the reach between CLB and SJP. The remaining 150 cfs must occur in the reach between SJP and VER. The model consistently under-predicted the salinity by as much as 300 umhos/cm during those periods.

Since there is a significant amount of flow missing, parameterizing Manning's 'n' would be premature at this juncture. The timing of the missing flow coupled with the discrepancy in the salinity leads to the conclusion that the missing water is from a poor quality source such as agriculture tail-water or groundwater base flow.

In order to proceed, a concept termed “add-water” was developed. Constant base flows of 200 cfs and 150 cfs were added to the boundary conditions just upstream of SJP and VER, respectively. HYDRO and QUAL Run18 correspond to the best calibration model run utilizing the add-water concept.

5.5.4.1 HYDRO

Since changes were only introduced downstream of CLB, the HYDRO Run18 results for NEW and CLB are not shown below because they are the same as HYDRO Run14a.

Minor improvement in simulated stage at SJP was achieved between Run14a and Run18 (see Figure 5-19). The MSS value decreased from 1.047 to 1.021 (see Figures 5-8 and 5-17), respectively. More improvement was achieved at VER (see Figure 5-19). The MSS value decreased from 1.009 to 0.731 (see Figures 5-9 and 5-18), respectively. Please note the scale difference of the Y-axis between the two plots in Figure 5-19.

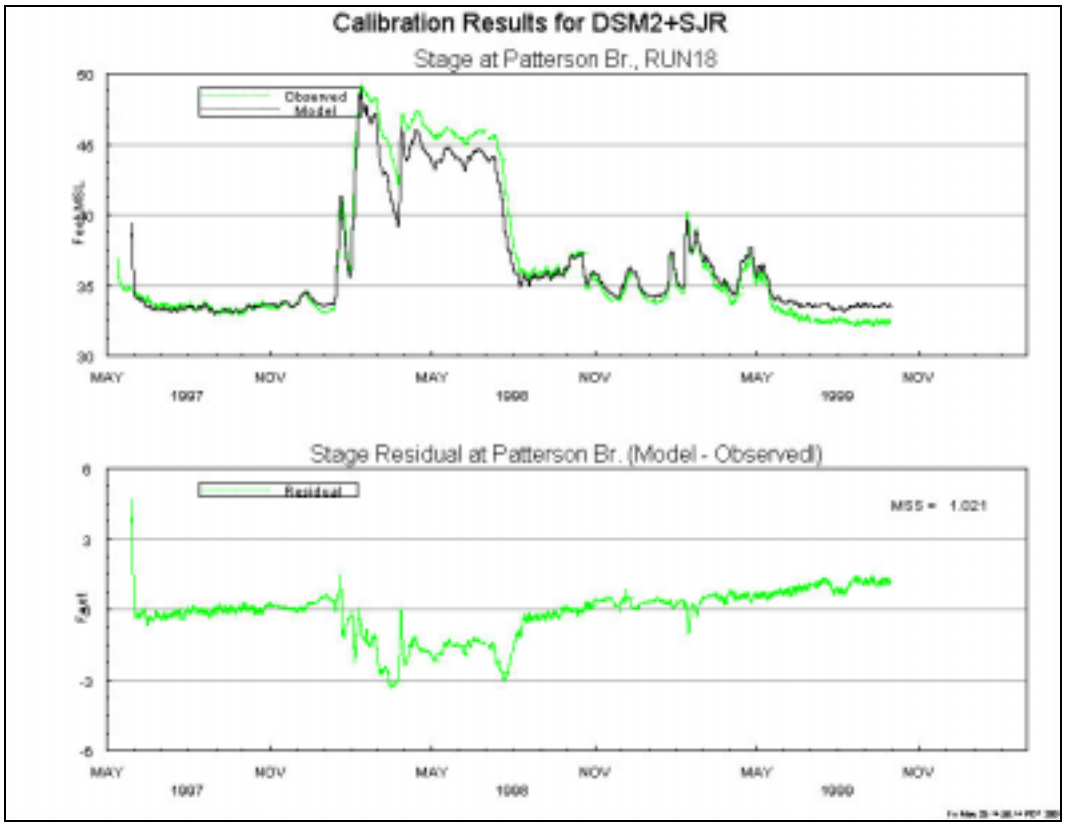

Figure 5-17: DSM2 Calibration Results for Stage at SJP.

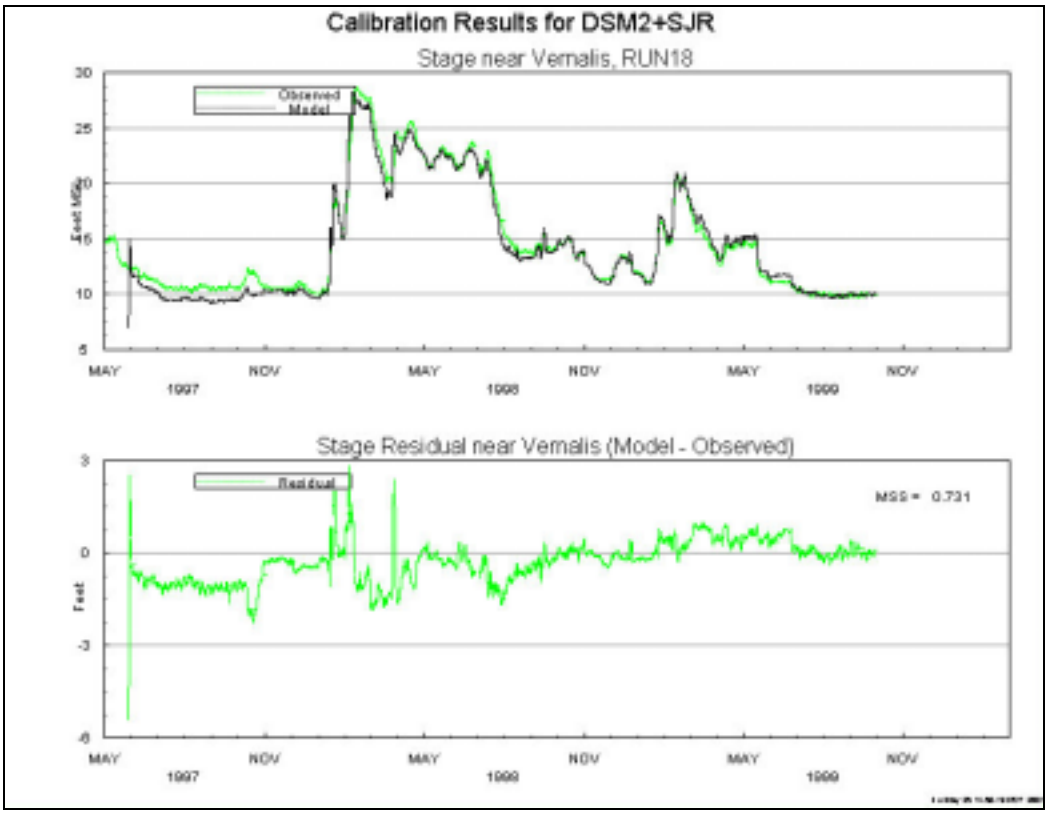

Figure 5-18: DSM2 Calibration Results for Stage at VER.

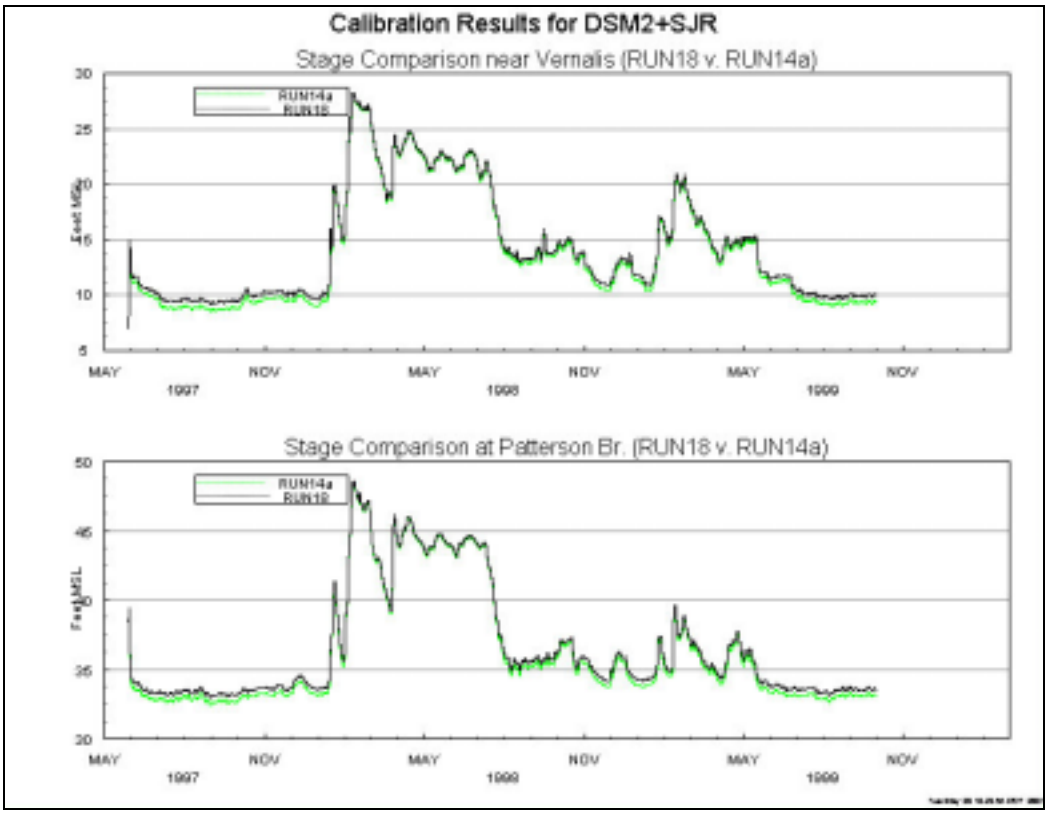

Figure 5-19: Comparison of Pre-Calibration and Calibration Stages at SJP and VER.

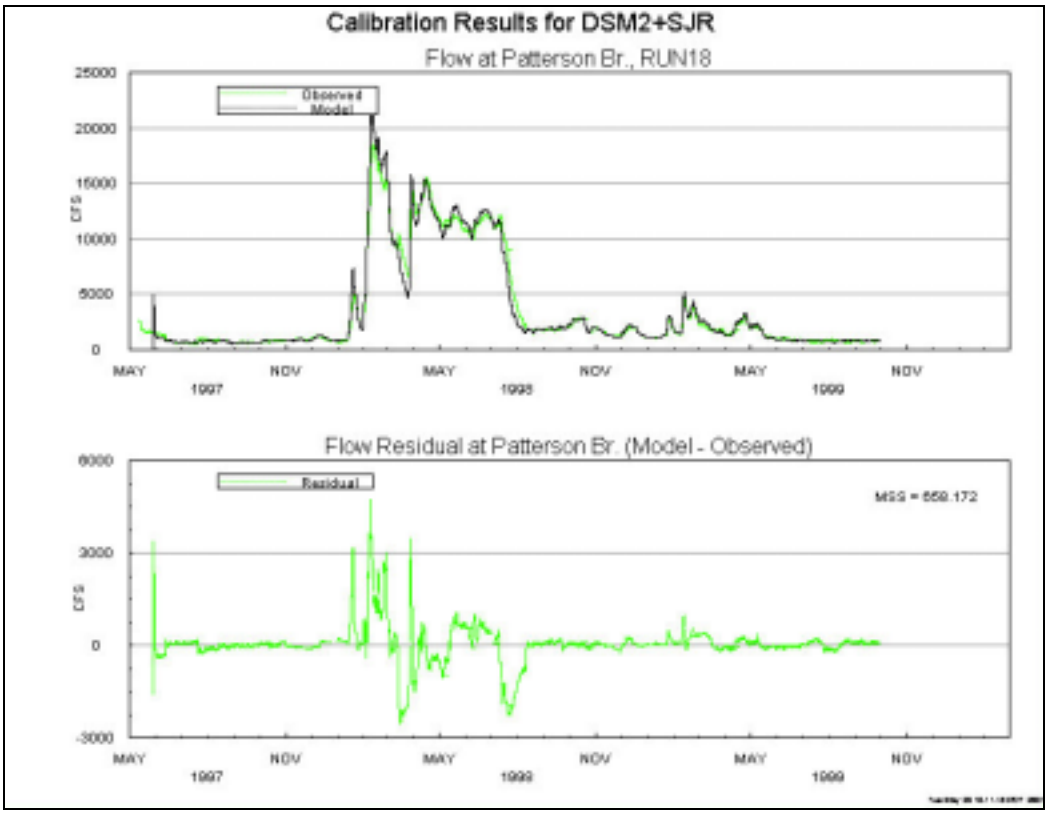

Figure 5-20: DSM2 Calibration Results for Flow at SJP.

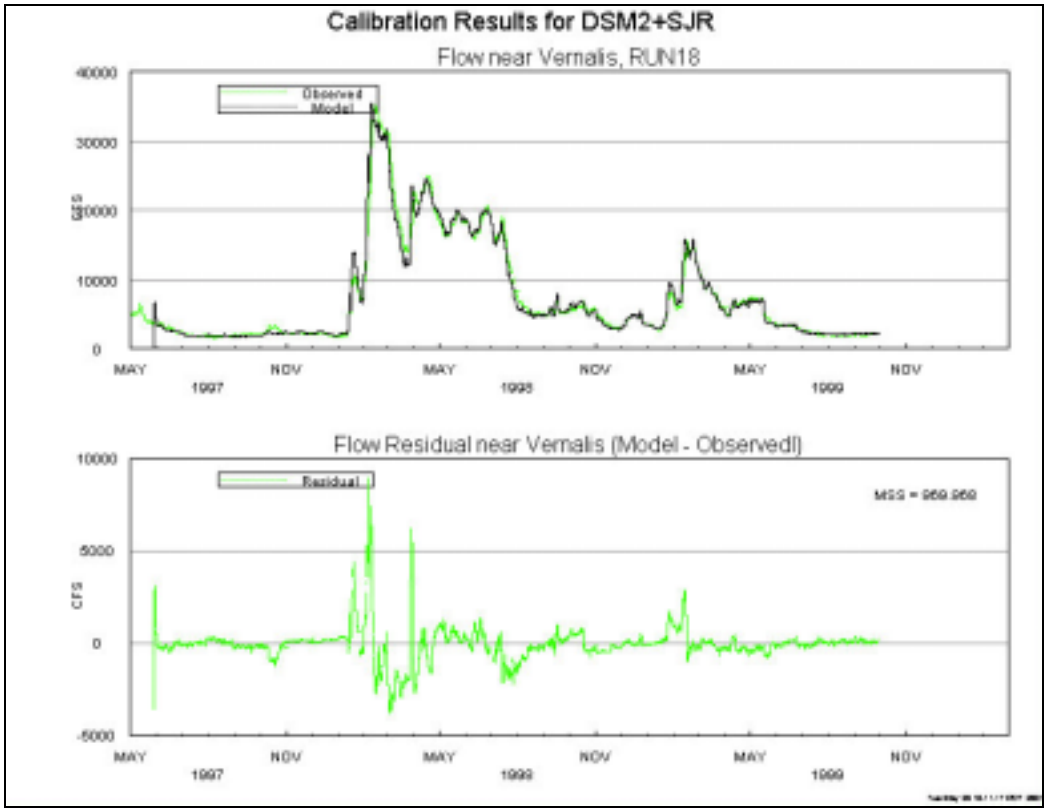

Figure 5-21: DSM2 Calibration Results for Flow at VER.

Significant improvement in simulated flow at SJP was achieved during the low-flow regime between Run14a and Run18 (see Figure 5-22). The MSS value decreased from 677.0 to 658.1 (see Figures 5-12 and 5-20), respectively. Significant improvement was also achieved at VER (see Figure 5-22). The MSS value decreased from 1042.5 to 969.9 (see Figures 5-13 and 5-21), respectively. Please note the scale difference of the Y-axis between the two plots in Figure 5-22.

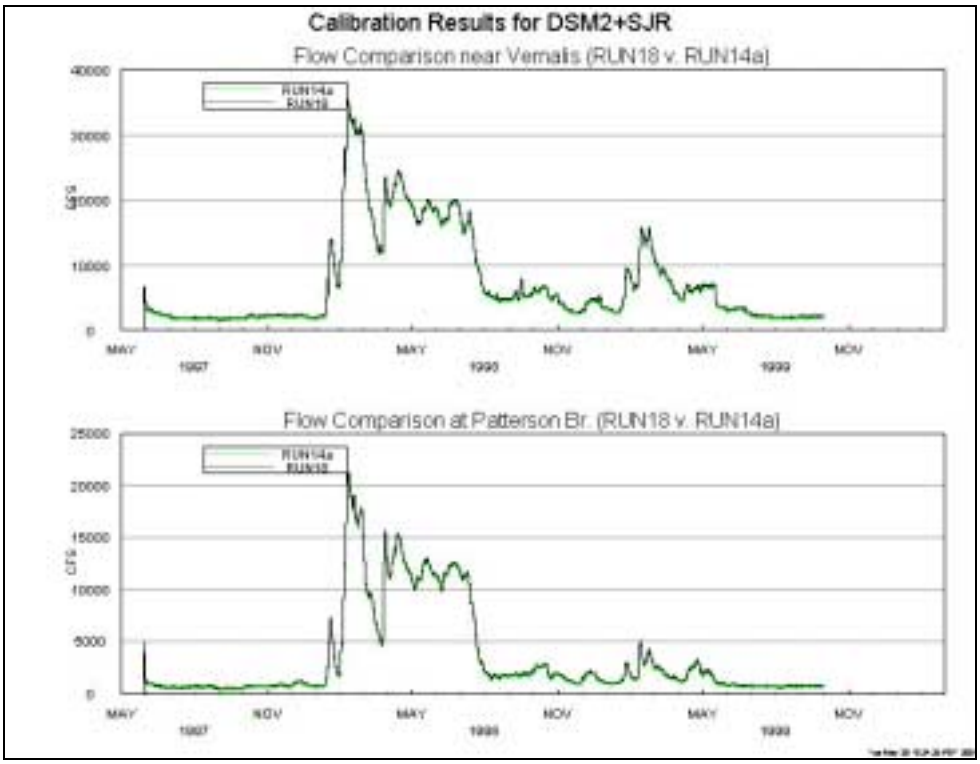

Figure 5-22: Comparison of Pre-Calibration and Calibration Flows at SJP and VER.

5.5.4.2 QUAL

Since changes were only introduced downstream of CLB, the QUAL Run18 results for CLB are not shown below because they are the same as QUAL Run14.

Now that a better flow match was achieved, a reasonable salinity trend needed to be determined to assign to the add-water. Due to the seasonal trend of the flow and salinity deficits, the temporal trend of an agriculture return appeared appropriate, but the magnitude needed to be higher than a typical agriculture return to improve the deficit. After some iteration, a salinity signature was developed with the temporal variability of an agriculture return and a magnitude consisting of a combination of 10% to 30% groundwater and 70% to 90% agriculture tail-water.

This salinity signature produced a significant increase in simulated salinity throughout the calibration period (see Figures 5-23 and 5-24). The MSS value between Run14 and Run18 was 123.9 to 75.7, respectively (a change of approximately 40%). The most significant changes were during the high-salinity regime with little change during the low-salinity regime. This trend is due to dilution of the poor quality add-water by high system flows.

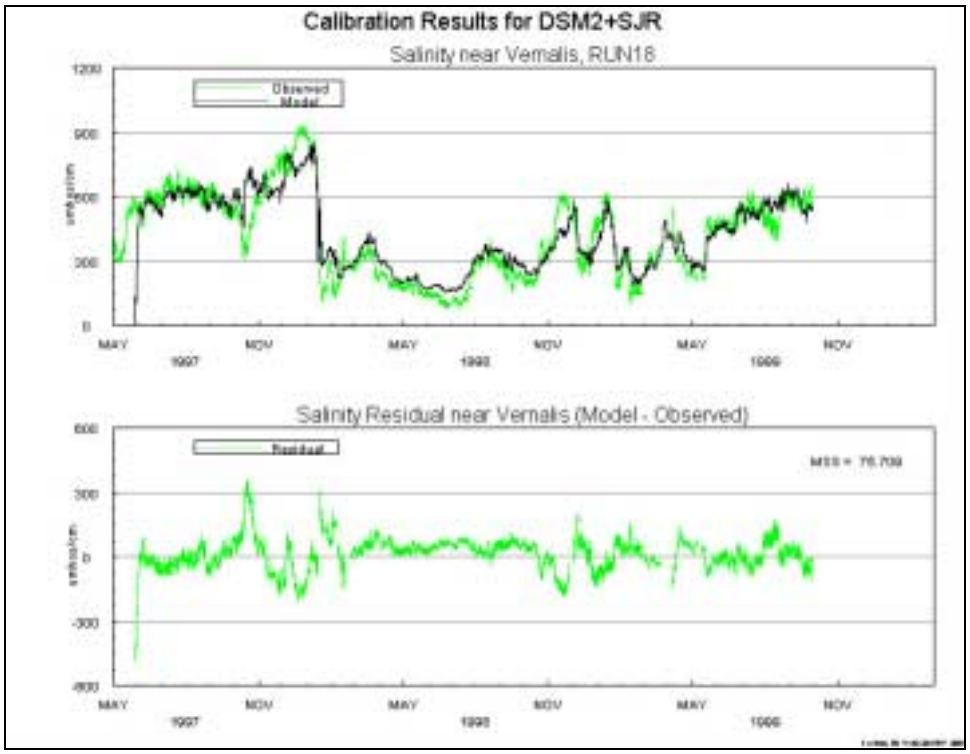

Figure 5-23: DSM2 Calibration Results for Salinity at VER.

Figure 5-24: Comparison of Pre-Calibration and Calibration Salinities at VER.

5.5.5 Discussion

Some of the inconsistencies between over- and underestimation of stage at the same location during the simulation period such as high and low flow regimes may be explained by scour and deposition phenomenon that occurs in the actual system but is not accounted for by DSM2. These processes can affect the modeling results because the changes in the channel bottom elevation will affect the field stage readings, but the model's channel bottom elevation is fixed and cannot compensate for the higher or lower field reading for the equivalent flow. Possible discrepancies between the field and model's estimated geometry of flood plain representation could also be a factor.

Flow discrepancies between the model and observed values may also be explained by scour and deposition phenomenon. Flows at gauging stations are obtained using developed rating curves that relate the river stage and static geometry to a flow value. These rating curves are not reevaluated as often as the cross section changes. Therefore, if the rating curve is developed for a particular cross section and the geometry of the section changes but the relationship is not updated, then the reported flow will not be accurate. These potentially inaccurate flows are then used as boundary conditions and calibration benchmarks. Possible discrepancies between the field and model's estimated geometry of flood plain representation could also be a factor in flow discrepancies.

Trend discrepancies between stage and flow at the same time and location lend further support to the scour and deposition effects in the simulation results. Sometimes, the stage will over-predict while the flow is under-predicted. Therefore, it may not be reasonable to expect a good match during these extreme flow event periods.

Preliminary investigation of the phase shift has led to suspicion that gage errors may be an important factor. More often than not, gauging stations tend to stop logging or log erroneous data during storm events. Many of the boundary conditions used for this historical study were missing flood peaks and sometimes the entire flood hydrograph. These missing hydrographs and flood peaks had to be estimated using engineering judgement for the most part. Another possible factor could be improper lagging of the eastside tributary flows. Since the gauging stations that provided the Stanislaus and Tuolumne River boundary flows are located approximately 15 miles upstream of the their confluence with the SJR, the flows seen at these gages will be seen at the confluences later in time. However, some sensitivity analysis of the lag factor has shown this may not be likely. The rating-curve, geometry, scour, and deposition issues mentioned previously could play a role here as well.

The major weaknesses in the boundary conditions are the westside agriculture and groundwater components borrowed from SJRIO. These relationships were developed almost 20 years ago from a very limited amount of information. The westside agricultural contribution is modeled by static relationships, which are thoroughly documented in Kratzer et al., 1987. Some of the assumptions used to develop these relationships may no longer be representative of the current state of the system. Many water districts have merged, agricultural practices have become more efficient, and land use has changed during that time. The groundwater component is too monotonous to be representative of wet and dry years alike. However, to improve upon the SJRIO assumptions will require a significant amount of time and information to justify changes.

Some new data sources for westside agriculture activities are being developed by the San Joaquin River Management Program Water Quality Subcommittee. Also, the Hospital/Ingram Creek watershed is completely ungaged and Del Puerto Creek does not have a salinity monitor in conjunction with flow measurement. These tributaries are important contributers of salinity to the SJR.

Some improved boundary condition data will be available in the future due to recent installations of new gauging stations. Salinity monitoring equipment was added at Tuolumne River and SJR near the Stevinson locations. The flow and salinity station at the Merced River location was rehabilitated. New salinity monitoring is proposed for the SJP and SJR at Maze Road locations. These additions will create more salinity calibration locations.

5.5.6 Conclusions

- The add-water concept can be used effectively to calibrate the DSM2 model. A longer historical simulation period is needed to refine the general assumptions to improve the add-water parameters.

- The current state of the DSM2 model is an effective tool for studies concerned with low-flow regime issues. Typically, the primary focus of studies in the SJR is during flow periods, so it is not critical for an excellent calibration match during high-flow periods at this time.

- There are some weaknesses in the boundary conditions that need improvements. The recent installation of some new stations will improve future simulations as new data become available.

- The empirical relationships inherited from SJRIO need to be replaced with observed data or the derivations updated.

5.6 Future Directions

- Develop an isolated SJR model (without the Delta) using the nonreflective Martinez stage boundary,

- Incorporate improved boundary conditions,

- Conduct a long-term historical validation,

- Plan study development and linking with CALSIM II,

- Extend model grid to the Eastside tributary reservoirs, and

- Extend Phase II to the Mendota Pool.

5.7 References

Kratzer, C.R., P.J. Pickett, E.A. Rashmawi, C.L. Cross, and K.D. Bergeron. (1987). *An Input-Output Model of the San Joaquin River from the Lander Avenue Bridge to the Airport Way Bridge.* Technical Committee Report No. W.Q. 85-1. California State Water Resources Control Board.